

RESEARCH

Open Access



Combination of transcriptome and Mendelian inheritance reveals novel prognostic biomarker of CTLA-4-related lncRNAs and protective role of nitrogen metabolism pathway in lung adenocarcinoma development

Huisi Shan^{1,2†}, Xiaocong Wang^{3†}, Fei Yin⁴, Yiting Zhou^{5,6}, Liuhan Mao⁵, Xiao Zhu^{5,7*} and Caixin Liu^{1*}

Abstract

Objective Since in the cancer setting, tumor cells may use cytotoxic T-lymphocyte-associated protein 4 (CTLA-4) to evade the immune system. This study aimed to identify CTLA-4-related long non-coding RNAs (lncRNAs) and assess their roles in lung adenocarcinoma (LUAD) development.

Methods Clinical and genomic data were obtained from The Cancer Genome Atlas (TCGA), MSigDB and Gene Weaver. CTLA-4-related lncRNA-based gene signatures (CTLA4LncSigs) were identified using Cox regression, establishing a risk score model and an independent prognostic model. Enrichment analysis (GO/KEGG) was performed. Mendelian randomization (MR) analysis investigated the nitrogen metabolism and lung cancer relationship, with Bayesian weighted MR (BWMR) addressing uncertainties. Correlations with tumor microenvironment and drug sensitivity were explored.

Results Nineteen CTLA4LncSigs significantly influenced LUAD prognosis. The risk score demonstrated independence as a prognostic factor. Functional analysis revealed lncRNAs' impact on nitrogen metabolism. MR and BWMR confirmed the protective role of the nitrogen metabolism pathway in lung cancer.

Conclusion Our study identifies CTLA-4-related lncRNAs associated with LUAD prognosis and uncovers a previously undiscovered protective role of the nitrogen metabolism pathway in combating LUAD development, providing new insights into potential therapeutic targets and prognostic biomarkers for this aggressive cancer subtype.

Keywords CTLA-4-related lncRNA-based signatures, Tumor microenvironment, Lung adenocarcinoma, Prognosis, Mendelian randomization

[†]Huisi Shan and Xiaocong Wang contributed equally to this work.

*Correspondence:

Xiao Zhu
xzhu@gdmu.edu.cn
Caixin Liu
liucaixin@yjsy.com

Full list of author information is available at the end of the article



Introduction

Cytotoxic T-lymphocyte-associated protein 4 (CTLA-4) is an immune checkpoint molecule expressed primarily on the surface of T cells. It regulates the immune response by inhibiting T-cell responses to prevent excessive immune responses [1]. Tumor cells may use CTLA-4 to evade the immune system. Recently, a new type of immunotherapy mediated by immune checkpoint inhibitors (ICIs) has emerged [2], which enhances the lethality of the adaptive immune system against cancer cells. Immune checkpoints are a set of cell surface receptors that suppress T cell functions in an activated state [3]. The Food and Drug Administration (FDA) has approved ICIs designed to target CTLA-4 as a treatment option for various cancer types [4, 5]. In 2021, M Reck et al. demonstrated that Nivolumab + ipilimumab + two cycles of chemotherapy are more effective than conventional chemotherapy for NSCLC patients [6].

The clinical benefit of therapeutic regimens can be predicted by biomarkers in addition to imaging and pathological examination [7]. Biomarkers can be measured in peripheral blood and stool [8, 9], and they have several potential advantages over tissue biopsy, such as being relatively noninvasive and repeatable [10]. Long non-coding RNAs (lncRNAs) play key roles in many cellular processes, including transcription, post-transcriptional regulation, and the cell cycle [11, 12].

Gathering evidence increasingly indicates that lncRNAs play a pivotal role in the development, advancement, and response to treatment in lung cancer [13–15], thereby offering valuable insights for clinical management. It has been predicted that specific lncRNAs regulate CTLA-4 thereby affecting breast cancer progression [16]. However, to date, no studies have investigated the prognostic value of CTLA-4-related lncRNA-based gene signatures (CTLA4LncSigs) in lung adenocarcinoma (LUAD) patients. In this study, we conducted a risk score model and an independent prognostic model. We gain insight into the expression and function of specific CTLA-4 related lncRNAs, evaluating their impact on immune regulation and tumor progression and putting forward some potential drugs. Furthermore, we discussed the protective role of nitrogen metabolism in LUAD by Mendelian randomization (MR) analysis. These validated our findings in transcriptome implying that CTLA4LncSigs is a novel prognostic biomarker of LUAD.

Experimental approach and procedures

Acquiring and refining data

For this study, we obtained five gene sets consisting of 405 genes associated with CTLA-4 from the Molecular Signatures Database (MSigDB), accessible at (<https://www.gsea-msigdb.org/gsea/msigdb>). The

immunologic signature collections of genes, namely “GSE37563_WT_VS_CTLA4_KO_CD4_TCELL_D4_POST_IMMUNIZATION_DN” ($n=183$) and “GSE37563_WT_VS_CTLA4_KO_CD4_TCELL_D4_POST_IMMUNIZATION_UP” ($n=165$), were included, along with the curated gene sets “BIOCARTA_CTLA4_PATHWAY” ($n=22$), “REACTOME_CTLA4_INHIBITORY_SIGNALING” ($n=21$) and “WP_CANCER_IMMUNOTHERAPY_BY_CTLA4_BLOCKADE” ($n=14$). After eliminating duplicates, we obtained a total of 382 genes. Additionally, we obtained 90 CTLA-4-related genes from Gene Weaver (<https://geneweaver.org>), which, when integrated with the 382 genes from MSigDB, yielded a total of 455 genes after removing duplicates [17]. We employed the “limma” package in R software (version 4.0.2; <https://cran.r-project.org/>) to identify lncRNAs exhibiting a correlation coefficient of 0.4 and $p < 10^{-53}$ with the gene sets. Subsequently, we employed univariate Cox regression analysis to screen out significant ($p < 0.05$) lncRNAs ($n=131$). We acquired gene expression, clinicopathological, and prognostic data for 494 LUAD patients from The Cancer Genome Atlas (TCGA). What’s more, we retrieved and obtained genetic data on blood urea nitrogen levels (ebi-a-GCST90103632, Sample size 173,149, Number of SNPs 7,777,636) and lung cancer (ebi-a-GCST004748, Sample size 85,716, Number of SNPs 7,857,154) via IEU Open GWAS project (<https://gwas.mrcieu.ac.uk/>) (Table S1).

Data grouping and prognostic analysis

To pinpoint lncRNAs linked to the overall survival (OS) of LUAD patients, we built a multivariate Cox regression analysis model based on univariate Cox regression analysis and the least absolute shrinkage and selection operator (LASSO) Cox regression analysis, which we called the risk score model. In this model, we can not only get CTLA4LncSigs, but also calculate the risk score of each patient. We also used this model to group 494 patients from the TCGA to ensure that there were no statistical differences in each clinicopathological factor between the training and testing datasets.

The risk score for each patient was computed utilizing the following formula in the model: $Risk\ score = \sum_{i=1}^n coef_{lncRNAi} \times exp(coef_{lncRNAi})$ ($coef$ indicates the regression coefficients, $exp(coef)$ indicates the expression level in LUAD patients) [18, 19]. By employing the median risk score as the threshold, we segregated LUAD patients in the training dataset into two distinct subgroups: the high-risk group and the low-risk group. Subsequently, we evaluated the OS of these two subgroups using the Kaplan–Meier method.

This study delved into exploring the correlation between the risk score and various clinicopathological factors, including gender, age, American Joint Committee

on Cancer (AJCC) stages, primary tumor (T), regional lymph nodes (N), and distant metastasis (M). To assess the impact of these factors and risk score on patient prognosis, we utilized univariate and multivariate Cox regression analyses to develop an independent prognostic model. The performance of this model was evaluated using receiver operating characteristic (ROC) curves and concordance index (C-index) curves. Furthermore, we employed a nomogram to visualize how to predict a patient's survival probability, which was assessed by the calibration curve. Moreover, we used the Kaplan–Meier method to compare the survival time of patients in the high-risk and low-risk groups with different clinicopathological factors [20, 21], so as to verify whether the risk score is predictive. Additionally, we performed principal component analysis (PCA) to investigate genetic differentiation between high-risk and low-risk subgroups.

The analyses encompassed the enrichment of gene ontology and the Kyoto encyclopedia of genes and genomes

To gain a deeper understanding of the role played by CTLA4LncSigs, we conducted a screening process to identify lncRNAs exhibiting significant differences in expression levels ($|\log_{2}FC| > 1$, $p < 0.05$) between high-risk and low-risk subgroups. Subsequently, we carried out enrichment analyses for Gene Ontology (GO) and the Kyoto Encyclopedia of Genes and Genomes (KEGG) pathways using R packages. In the Fisher exact test, the p-values for GO and KEGG were corrected for false discovery rate (FDR) and found to be below 0.05 and 0.3, respectively, signifying the significance of these indicators.

Analysis of tumor microenvironment

We employed Gene Set Variation Analysis (GSVA) to examine CTLA4LncSigs and assess the disparity in immune function-related expression associated with CTLA4LncSigs between the high-risk and low-risk subgroups.

Tumor Mutation Burden (TMB) quantifies the cumulative count of somatic gene coding errors, base substitutions, gene insertions, or deletions identified per million base pairs [22]. Several investigations have provided evidence that individuals with elevated TMB experience notably increased response rates and extended periods of progression-free survival compared to individuals with lower TMB levels [23]. We conducted a comparison of TMB between the high-risk and low-risk subgroups and illustrated the outcomes through survival curves.

Next, we analyzed tumor immune escape and immunotherapy of CTLA4LncSigs using the Tumor Immune Dysfunction and Exclusion (TIDE) web platform, which

can infer the role of genes in regulating tumor immunity and evaluate biomarkers to predict ICI clinical response. In particular, we acquired TIDE scores for 494 patients diagnosed with LUAD using the TIDE web platform (<http://tide.dfci.harvard.edu/>). Our analysis encompassed a range of immune biomarkers and cell factors, which included IFNG [24], Microsatellite Instability (MSI) score [25], Merck18, CD274/PD-L1 [26], CD8 [27], Myeloid-derived suppressor cell (MDSC) [28], immune exclusion, immune dysfunction, cancer-associated fibroblasts (CAF) [29] and tumor-associated macrophages M2 (TAM M2) [30].

Exploring available drugs

To identify potential drug candidates for LUAD patients, we employed the "pRRophetic" package within R software to estimate the semi-inhibitory concentration (IC50) of a variety of chemotherapy drugs sourced from the Genomics of Drug Sensitivity in Cancer (GDSC) database. We then analyzed the drug responses in both the high-risk and low-risk subgroups.

Mendelian randomization analysis

Nitrogen metabolic pathways derived from KEGG are closely related to CTLA-4LncSigs. To assess the link between CTLA-4LncSigs and LUAD, we explored whether there is a relationship between nitrogen metabolic pathways and LUAD. The data from IEU Open GWAS project were subjected to a 2-sample Mendelian randomization (2SMR) analysis [31]. We used the inverse-variance weighted (IVW) method as the leading analysis while the MR-Egger regression method was used to perform the pleiotropic test. Leave-One-Out Mendelian Randomization (LOO MR) was used to assess the impact of each SNP on the outcome. We took into account the uncertainty of the estimated weak effects and the possible bias in MR analysis through Bayesian weighted Mendelian randomization (BWMR) based on the following formula: $P(\beta|data) = \frac{P(data|\beta)P(\beta)}{P(data)}$ (β indicates the causal effects of genes on exposure and outcomes.) [32].

Statistical analysis

Statistical analysis and figure plotting were conducted using the R software. The OS was presented through the Kaplan–Meier curve. A significance level of $p < 0.05$ was used to denote statistical significance.

Results

Identifying lncRNAs associated with CTLA-4

Using univariate Cox regression analysis, we identified 131 lncRNAs with p values less than 0.05, among which

high-risk subgroup exhibited significantly lower survival time and rate in comparison to those in the low-risk subgroup ($p < 0.001$) (Fig. 1C-F). The heatmap of the training dataset demonstrated differential expression of CTLA4LncSigs between high-risk and low-risk subgroups. AC010999.2, ERCC8-AS1, and AC104971.3 were highly expressed in the low-risk subgroup, indicating their tumor-protective role. Conversely, AP000253.1 and FAM66C were highly expressed in the high-risk subgroup, indicating their role as tumor risk factors (Fig. 1F).

We assessed the precision of the outcomes obtained from the training dataset by examining the testing ($n = 164$) and entire datasets ($n = 494$) using the same approach. At the outset, we stratified both the testing dataset ($n = 84$) and the entire dataset ($n = 249$) into high-risk subgroups, along with low-risk subgroups (testing dataset $n = 80$; entire dataset $n = 245$), using the median risk score as the criterion. The Kaplan–Meier survival curves for both the testing dataset ($p = 0.019$) and the entire dataset ($p < 0.001$) mirrored those observed in the training dataset, affirming that individuals in the high-risk subgroup experienced notably shorter survival times compared to those in the low-risk subgroup (Figure S1A-B). Furthermore, the survival rate among LUAD patients within the high-risk subgroup was notably lower than that within the low-risk subgroup, a trend consistently observed in both the testing and entire datasets. These findings align with the results obtained from the training dataset (Figure S1C-F). The heatmap of the testing and entire datasets revealed that AC010999.2, ERCC8-AS1, and AC104971.3, the protective factors, were highly expressed in low-risk areas, while AP000253.1 and FAM66C, the risk factors, were highly expressed in high-risk areas (Figure S1G-H). These findings suggest that the risk score can accurately predict the survival outcome of LUAD patients.

Relationship between risk score and clinicopathological factors

According to the risk score model we had developed previously, we calculated the risk score of each patient through following formula: $Risk\ score = \sum_{i=1}^n coefIncRNAi \times \exp(coef)IncRNAi$ (coef indicates the regression coefficients, $\exp(coef)$ indicates the expression level in LUAD patients). Patients were stratified into high-risk and low-risk groups based on the median risk score. We further investigated the relationship between clinicopathological factors and risk score and found that the later the clinical stage of the tumor, the higher the risk score (Figure S2A-C). There was a positive correlation between the risk score and the survival status of patients (Figure S2D). However, age ($p = 0.8$), race ($p > 0.05$), gender ($p = 0.5$), and M ($p = 0.7$) had no significant associations with risk

score (Figure S2E-H). We infer that the sample size and statistical power of our study might not be sufficient to detect subtle differences linked to these clinicopathological factors. Larger cohorts could help elucidate these associations more clearly.

Establishment and evaluation of independent prognostic model

Following the application of the independent prognostic model, which was built through both univariate (Fig. 2A) and multivariate Cox regression analysis within the entire dataset, our findings indicated that among variables such as age, gender, race, AJCC stage, T, M, N, and risk score, only the risk score exhibited a statistically significant association ($p < 0.05$) with the survival time of LUAD patients (Fig. 2B).

ROC curve illustrated that the model demonstrated strong predictive performance for estimating the survival rate of LUAD patients (1-year area under the curve, $AUC = 0.762$, 3-year $AUC = 0.773$, 5-year $AUC = 0.787$, as shown in Fig. 2C). When it comes to forecasting the 5-year survival rate of LUAD patients, the following factors exhibited significance with AUC values greater than 0.5: risk score ($AUC = 0.787$), race ($AUC = 0.543$), AJCC stage ($AUC = 0.646$), T status ($AUC = 0.594$), the M ($AUC = 0.524$), and N involvement ($AUC = 0.626$). This is depicted in Fig. 2D. The prognostic determinants for the 1-year and 3-year survival rates are depicted in Fig. 2E, F, respectively. In summary, the risk score emerged as the most robust predictor of LUAD patient survival, with other factors potentially serving as supplementary indicators. The C-index curve indicated that the risk score, AJCC stage, T, and N could still be utilized as predictors of the survival rate of LUAD patients (index > 0.5), whereas the indices of other factors were close to 0.5 (Fig. 2G). This outcome was by the ROC curve's forecast.

We created a nomogram utilizing the independent prognostic model to efficiently estimate a patient's OS at 1, 3, and 5 years, as depicted in Fig. 2I. The nomogram's reliability was validated through the calibration curve (Fig. 2H).

In general, our independent prognostic model demonstrates strong capability in predicting the prognosis of LUAD patients.

Validating the reliability of risk score

By comparing the survival times of patients in the high-risk and low-risk subgroups with different clinicopathological factors, we can validate the reliability of risk score. As demonstrated by a series of Kaplan–Meier survival curves (Figure S3), patients in the high-risk subgroup with the following clinicopathological factors had significantly ($p < 0.05$) shorter survival rates than those in the low-risk

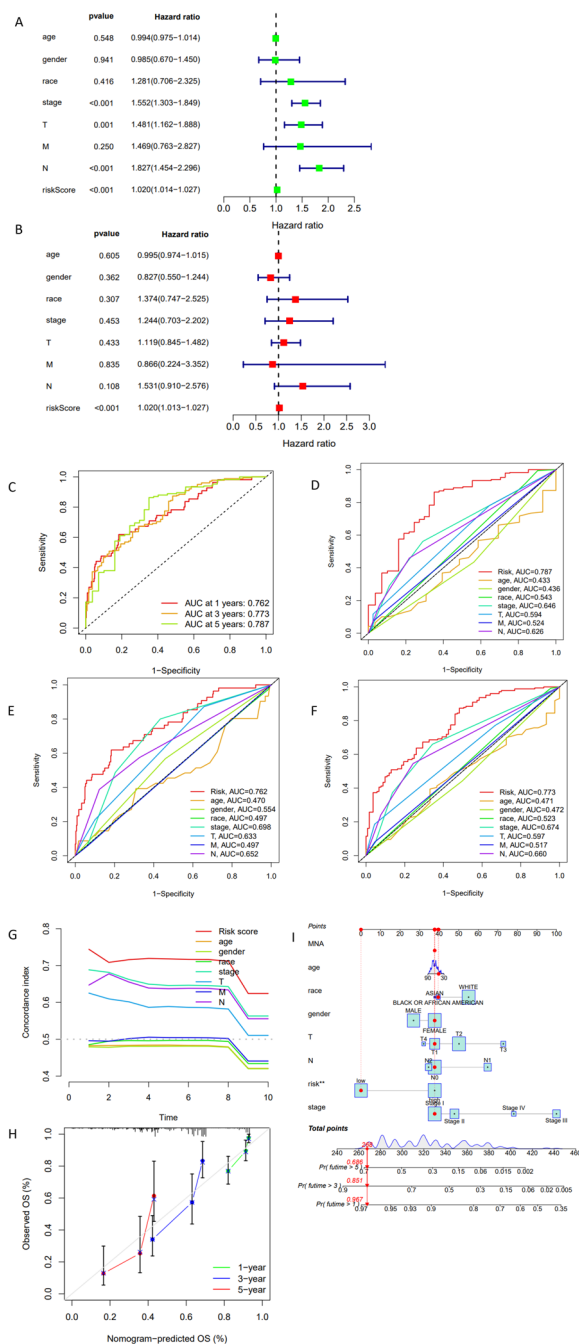


Fig. 2 The Result of Independent Prognostic Model in Entire Dataset. **A** is the forest map of univariate Cox regression analysis. **B** is the forest map of multivariate Cox regression analysis. The ROC curve of independent prognostic model for predicting 1, 3 and 5 years survival rates (**C**). The ROC curves of each clinicopathological factor and risk score for predicting 1 (**E**), 3 (**F**), 5 (**D**) years survival rates. The C-index curve of prognostic factors (**G**). Calibration curve evaluating the nomogram (**H**). The nomogram of predicting patients' survival rates. "***" means that the P value is less than 0.01 (**I**). The specific steps of using a nomogram are as follows: First, find the position of clinicopathological factors of the patient in the nomogram. Then, find their vertical counterparts on "Points" at the top of the nomogram. The number is the score for an individual factor. Add the scores of all factors to get the "Total points". "Total points" at the bottom correspond to the 1-year, 3-year, and 5-year survival rates of the patient

subgroup: patients under 65 years ($p=0.027$, Figure S3A), patients over 65 years ($p<0.001$, Figure S3B), male patients ($p=0.003$, Figure S3C), female patients ($p<0.001$, Figure S3D), white patients ($p<0.001$, Figure S3E), Asian patients ($p=0.046$, Figure S3T), patients with stage I ($p=0.006$, Figure S3F) and II ($p=0.01$, Figure S3G), patients with N0 ($p<0.001$, Figure S3H) and N1 ($p=0.036$, Figure S3I), patients with T2 ($p<0.001$, Figure S3J) and patients with M0 ($p<0.001$, Figure S3K). However, the survival rate of patients with T1 ($p=0.579$, Figure S3L), T3 ($p=0.089$, Figure S3M), and T4 ($p=0.644$, Figure S3N), patients with stage III ($p=0.306$, Figure S3O) and IV ($p=0.444$, Figure S3P), patients with M1 ($p=0.444$, Figure S3Q), patients with N2 ($p=0.696$, Figure S3R) and black or African American patients ($p=0.071$, Figure S3S) were not associated with the risk score. We hypothesize that this is due to the small sample size, e.g., only 13 cases for T4 and 18 cases for both stage IV and M1. Since Asian had only 6 cases, its results also need to be considered carefully. Overall, survival times for high- and low-risk patients differed significantly across most clinicopathological groups. Thus the risk score has prognostic value.

We analyzed differences in LUAD's genes (Figure S4A), LUAD's mRNAs (Figure S4B), LUAD's lncRNAs (Figure S4C), and CTLA4LncSigs (Figure S4D) in high- and low-risk patients by PCA. All these plots showed clear separation between high-risk and low-risk groups. This indicated that the expression profiles of CTLA-4-related lncRNAs can effectively distinguish between these groups, suggesting distinct genetic characteristics associated with different risk levels. The distinct clustering observed in PCA implies underlying genetic heterogeneity between high-risk and low-risk groups. This heterogeneity may be driven by differential regulation of CTLA-4-related lncRNAs, which in turn could influence tumor behavior and patient prognosis.

This reinforces the potential of CTLA-4-related lncRNAs as biomarkers for predicting patient outcomes and tailoring personalized treatment strategies.

Functional annotation and classification of lncRNA GO/KEGG

The GO functional analysis encompassed three distinct categories: biological process (BP), cellular component (CC), and molecular function (MF) (Fig. 3A). The findings indicated that among the lncRNAs, 22 BP terms, 25 CC terms, and 12 MF terms exhibited statistical

significance ($p < 0.05$, with FDR correction also $p < 0.05$). The mainly enriched BP terms were cornification, epidermis development and aging. The mainly enriched CC terms were cell-cell junction, intermediate filament and apical plasma membrane. The mainly enriched MF terms included alpha-catenin binding, enzyme inhibitor activity and extracellular matrix structural constituent. The relationship between lung cancer and apical plasma membrane and aging has also been found in other study [33]. Extracellular matrix structural constituent was linked to

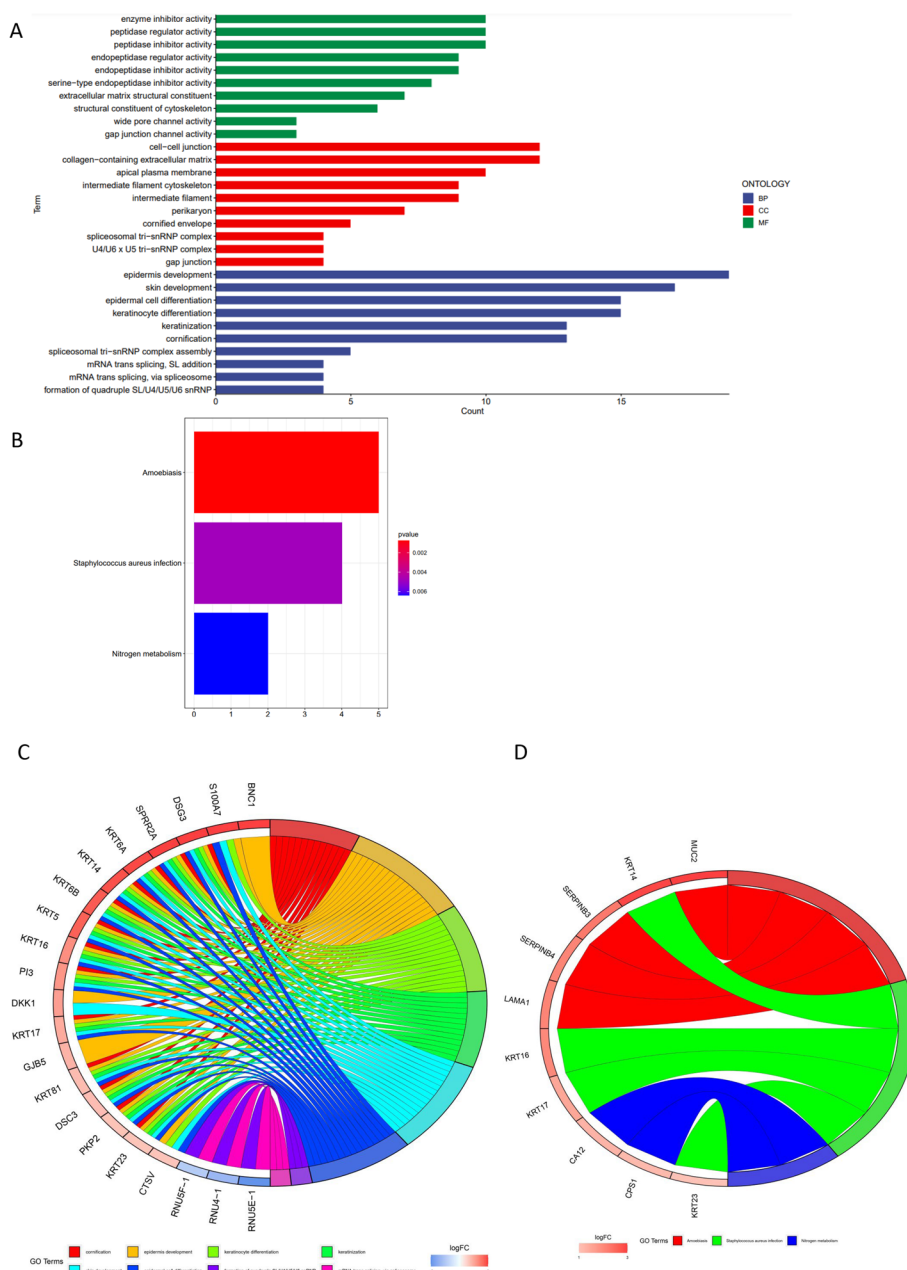


Fig. 3 The result of all differential lncRNAs ($n = 240$) between high-risk and low-risk subgroups in GO/KEGG. **A** and **C** are the results of the GO analysis. **B** and **D** are the results of the KEGG analysis

lung metastasis in colorectal cancer [34, 35]. Cell–cell junction is conducive to the collective invasion of tumor cells [36].

Hence, it is plausible that lncRNAs associated with CTLA-4 could potentially contribute to the invasion of lung cancer cells.

Subsequently, KEGG enrichment pathway analysis uncovered 3 significantly ($p < 0.05$, FDR corrected $p < 0.3$) enriched pathways (Fig. 3C), namely Amoebiasis, Staphylococcus aureus infection, and Nitrogen metabolism, with their corresponding lncRNAs shown in Fig. 3D. As cancer tissue has a much higher nitrogen requirement than non-proliferating normal tissue, regulating nitrogen metabolism may represent a potential cancer treatment [37, 38]. In conclusion, the inhibition of (CTLA-4)-related lncRNAs can effectively disrupt the nutrient supply to tumor tissue, thereby inhibiting tumor growth.

Assessment of immune function in high-risk and low-risk subgroups

The expression levels of lncRNAs associated with 13 immune functions were analyzed using a heat map (Figure S5) in both high-risk and low-risk subgroups. These functions encompassed APC co-inhibition, APC co-stimulation, CCR, checkpoint, cytolytic activity, HLA, inflammation promotion, MHC class I, parainflammation, T cell co-inhibition, T cell co-stimulation, type I IFN response, and type II IFN response [39]. The heat-map showed that cytolytic activity and human leukocyte antigen (HLA) in all datasets were highly expressed in the low-risk subgroup, suggesting that they are the protective factors. Similar findings were shown in patients with squamous cell carcinoma of the oral tongue, where high immune cytolytic activity was associated with a better prognosis [40]. Reduced antigen presentation due to low expression of HLA promotes immune escape [41]. Parainflammation displayed a higher expression in high-risk subgroup which is a procarcinogenic inflammatory process [42]. These observations suggest that immune functions are strong related to risk score.

Survival analysis of TMB

Additionally, we conducted a comparison of TMB between the high-risk and low-risk subgroups and observed no statistically significant distinctions ($p < 0.05$) in the training dataset ($p = 0.44$), testing dataset ($p = 0.91$), and the entire dataset ($p = 0.47$) (Figure S6A-C). Furthermore, there was no significant relationship ($p < 0.05$) between TMB and OS of LUAD patients in the training dataset ($p = 0.066$), testing dataset ($p = 0.184$), and the entire datasets ($p = 0.056$) (Figure S6D-F). Nonetheless, the combination of TMB and the risk score yielded a notable influence on the OS of LUAD patients (Figure

S6G). While the outcomes in the testing dataset (Figure S6H) and entire datasets (Figure S6I) displayed slight variations compared to the training dataset, it remained consistent that patients with high TMB and low-risk scores continued to exhibit the longest survival.

Analysis of tumor immune escape and immunotherapy of CTLA4LncSigs

We conducted an analysis and visualization of tumor immune escape and immunotherapy for (CTLA-4)-related lncRNAs in high-risk and low-risk subgroups. Figure 4 illustrates that the TIDE scores of the testing dataset ($p < 0.01$, **) and entire datasets ($p < 0.05$, *) were lower in the high-risk subgroup compared to the low-risk subgroup, indicating that lower TIDE scores correspond to higher risk scores, which is an unexpected finding (Fig. 4A b-c). However, the result in the training dataset was not significant (Fig. 4A a). Across the training, testing, and entire datasets, there was a notable increase in the presence of MDSC and CAF within the high-risk subgroup as compared to the low-risk subgroup. This suggests a correlation wherein higher levels of MDSC (Fig. 4B a-c) and CAF (Fig. 4C a-c) align with elevated risk scores. Other immune markers, such as MSI (Fig. 4D a-c), CD274 (Fig. 4E a-c), CD8 (Fig. 4F a-c), TAM M2 (Fig. 4G a-c), immune dysfunction (Fig. 4H a-c), Merck 18 (Fig. 4I a-c), immune exclusion (Fig. 4J a-c) and IFNG (Fig. 4K a-c), are also presented in the figures.

Drug selection for CTLA4LncSigs

To pinpoint potential chemotherapy drugs for CTLA4LncSigs, we employed the "pRRophetic" package with R software to assess drug responses within both high-risk and low-risk subgroups across the training, testing, and entire datasets. We identified 67 drugs in the training dataset, 59 in the testing dataset, and 77 in the entire dataset with significantly different estimated IC50 values between the high-risk and low-risk subgroups. Most drugs exhibited lower IC50 values in the high-risk subgroup. A subset of these drugs is presented in Figure S7A-L. IC50 of Erlotinib is lower in high-risk group than in low-risk group (Figure S7I). We inferred that it is related to FAM66C, one of the CTLA4LncSigs. FAM66C has a negative correlation ($HR > 1$) which means it is a risk factor for LUAD. High expression of FAM66C activates EGFR-ERK signaling by inhibition of the proteasome pathway promoting tumor growth [43]. Erlotinib is a specific inhibitor that targets EGFR and inhibits EGFR phosphorylation to block EGFR-ERK signaling [44]. Therefore, the IC50 of Erlotinib is lower in the high-risk group. Conversely, only a few drugs, such as BI.2536 and BIRB.0796 in the training dataset (Figure S7M-N), Methotrexate in the testing dataset (Figure S7O), and

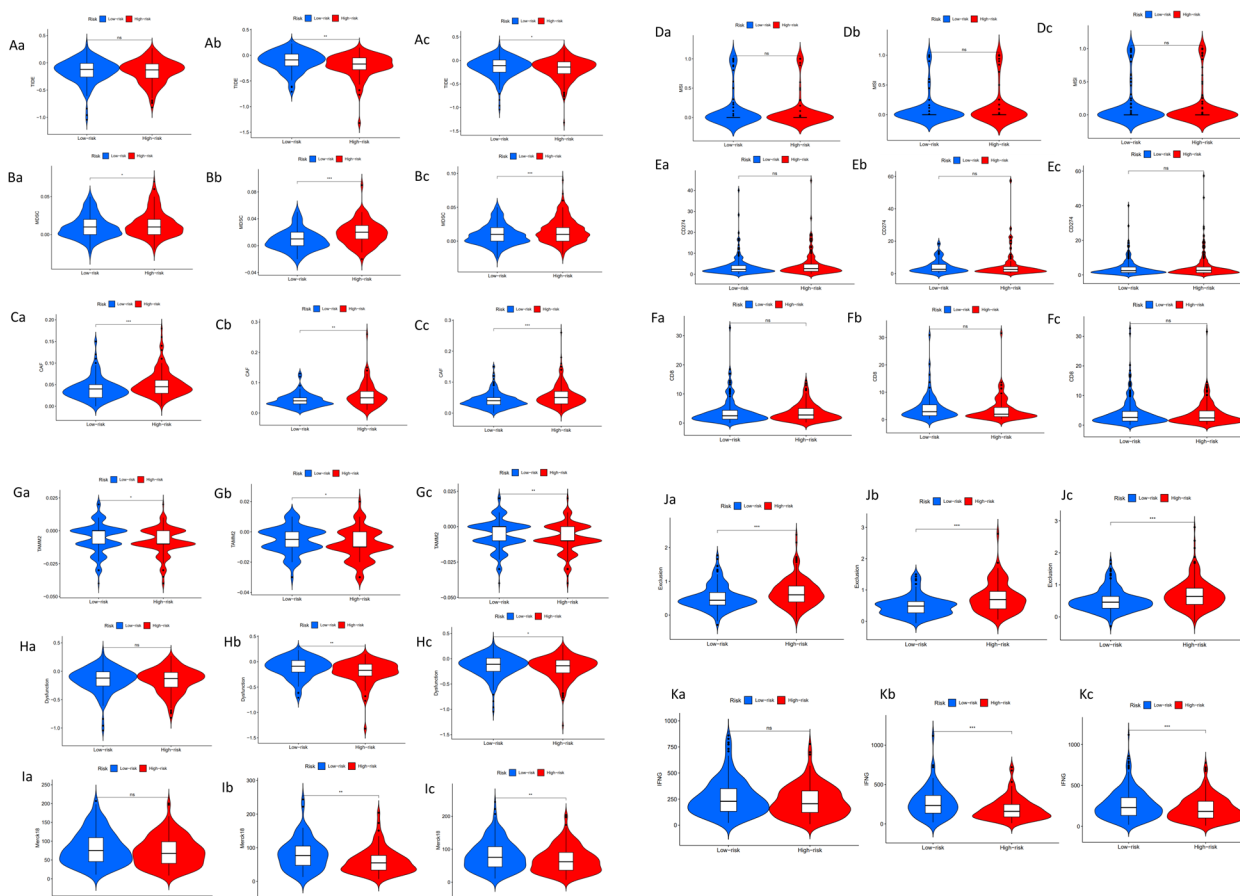


Fig. 4 The differences of tumor markers in high-risk and low-risk subgroups. Among them, “_a” means in the training dataset, “_b” means in the testing dataset, and “_c” means in the entire dataset. “*” means that $p < 0.05$, “**” means that $p < 0.01$, “***” means that $p < 0.001$, “ns” means no significant

Lenalidomide, Methotrexate, and PD.0332991 in the entire dataset (Figure S7P-R), exhibited greater sensitivity in the low-risk subgroup. These indicate that the risk score is strongly associated with IC50 so we can apply different drugs according the risk score, thereby supporting personalized treatment strategies. We suggest future research directions to validate these findings in larger, independent cohorts and experimental studies. This could include functional assays to elucidate the role of CTLA-4-related lncRNAs in mediating drug sensitivity and resistance.

Causal effects of nitrogen metabolism on lung cancer

The result of IVW indicated that blood urea nitrogen levels were significantly associated with lung cancer ($p < 0.05$) (Table S7). Meanwhile, the pleiotropic test showed no notable horizontal bias in 2SMR results ($p > 0.05$), which expressed that our 2SMR results were reliable (Table S6). The line direction of these methods is from top left to bottom right and roughly the same, which

means that the nitrogen metabolic pathway is a protective factor for lung cancer (Fig. 5A). The number of black dots on both sides of the line is roughly the same, which indicates that the results obtained by the IVW method are reliable (Fig. 5B). Figure 5C also showed the combined effect of these SNPs on lung cancer is protective in the IVW method. The results of LOO MR (Fig. 5D) indicated that MR analysis was not affected by an individual SNP, that is, MR sensitivity analysis was qualified.

Evidence Lower Bound (ELBO) is an indicator used to measure the quality of the data fitted to a model. The ELBO tends to a constant, indicating that the model has converged, and the model has a high degree of fitting to the data, that is, there is a strong causal relationship between the model and lung cancer (Fig. 5E). A high weight indicates that the observations conform to the assumptions of the instrumental variables and that the estimates of causal effects are reliable. In Fig. 5G, almost all observations have a high weight, indicating that these observations contribute significantly to estimates of

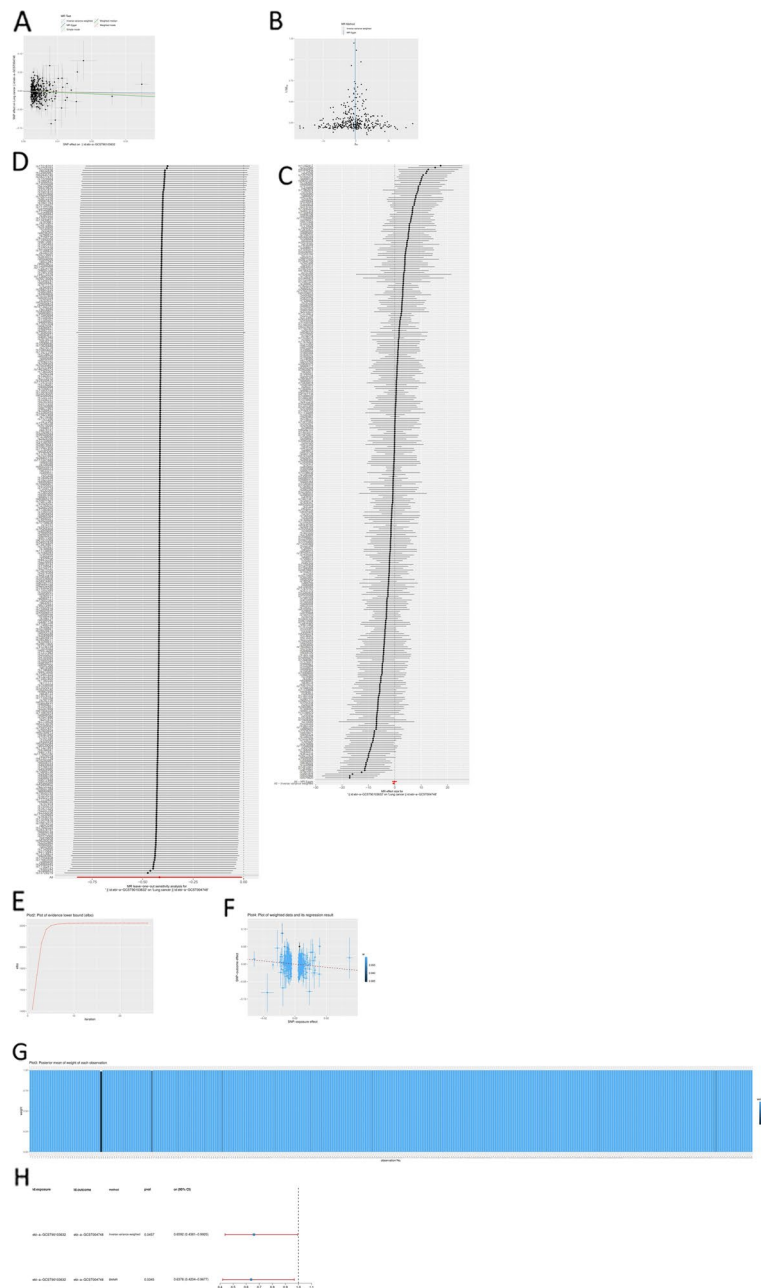


Fig. 5 The illustration of the MR Method. **A, B** further demonstrated that the 2SMR analysis results were dependable. The effects of each SNP on lung cancer are shown in **(C)**. The results of LOO MR **(D)**. The ELBO curve **(E)**. The observations are consistent with the hypothesis of the instrumental variables, and the estimation of the causal effect is reliable **F**. The posterior mean of the weight of each observation is close to 1, indicating that these observations contribute highly to the estimate of causal effects **(G)**. The odds ratios of MR and BWMR **(H)**

causal effects. Regression results of SNP-exposure and SNP-outcome effects for each observed value confirmed a significant association between nitrogen metabolism and lung cancer (Fig. 5F).

The odds ratio of the IVW method and BWMR analysis were both less than 1 ($p < 0.05$), suggesting that nitrogen metabolism was a protective factor for lung cancer

(Fig. 5H). KEGG showed that nitrogen metabolic pathway includes nitrification. High doses of the nitrification inhibitor Nitrapyrin cause liver tumors in mice [45, 46]. Overall, the results of MR Analysis showed a significant association between nitrogen metabolic pathways and lung cancer, indicating that our model is dependable.

Discussion

In recent decades, lung cancer has remained a significant cause of morbidity and mortality. Present diagnostic techniques, including imaging and pathological biopsy, exhibit constraints in predicting the prognosis of cancer patients on a large scale. In this study, we initially identified CTLA4LncSigs associated with prognostic risk signatures. We observed the lncRNAs AP000253.1 and FAM66C displayed higher expression levels in the high-risk subgroup, indicating their association with increased tumor risk. It is worth noting that these lncRNAs have been found to play diverse roles in previous studies [47, 48]. For instance, FAM66C was found to inhibit the proliferation of pancreatic cancer cells [49], while paradoxically promoting the proliferation of prostate cancer cells [50]. Although no effect of high or low-risk scores on patient response to medication was observed, risk score models based on CTLA4LncSigs were superior to clinicopathological factors in predicting efficacy.

GO functional analysis revealed that the mainly enriched BP terms were cornification, epidermis development and aging. The mainly enriched CC terms included cell–cell junction and apical plasma membrane. MF terms mainly enriched extracellular matrix structural constituent. The favorable effect of cell–cell junction on the collective invasion of tumor cells has been demonstrated [30]. Past research has already established the connection between lung cancer and apical plasma membrane and aging [33]. Extracellular matrix structural constituent was associated with lung metastasis in colorectal cancer [34, 35]. Subsequently, KEGG enrichment pathway analysis revealed three significant enrichment pathways for amoebic infection, *Staphylococcus aureus* infection, and nitrogen metabolism. It has been observed that nitrogen metabolism in cancer tissues differs significantly from that in normal tissues. The demand for nitrogen is significantly increased in rapidly proliferating tumor cells. Nitrogen plays a key role in the malignant progression of cancer [37, 38].

The results of MR Analysis also confirmed that the activity of the nitrogen metabolism pathway is a protective factor for lung cancer. KEGG showed that nitrogen metabolic pathway includes nitrification. High doses of the nitrification inhibitor Nitrapyrin cause liver tumors in mice [45, 46]. An active nitrogen metabolism pathway leads to an increase in glutamate production. Then accumulated glutamate enhances ferroptosis after the inhibition of system Xc⁻, and ultimately LUAD cells were sensitized to ferroptosis [51]. In addition, carbamoyl-P in the nitrogen metabolism pathway is involved in arginine biosynthesis. Arginine is essential for T cell survival, proliferation and functional expression [52].

Elevated arginine levels affect T-cell activation, differentiation, and function, resulting in better antitumor activity [53–55]. At the same time, the active nitrogen metabolic pathway also promotes the transformation and excretion of ammonia. Ammonia, as a metabolic waste, not only induces T-cell failure but also promotes tumor growth [56]. Ammonia can also be taken up by some cancer cells as a biosynthetic metabolite to drive amino acid metabolism [57]. These discoveries imply a strong link between lncRNAs related to CTLA-4 and the onset and progression of cancer. The predictive ability of lncRNA deserves further study.

It is undeniable that alterations in the tumor microenvironment play a crucial role in cancer progression. We identified a cluster of immune-function pathways: checkpoint and T cell co-stimulation, which we show are linked to low risk of tumor. These pathways also play a similar role in genes associated with Solute carrier transporters (SLC) in osteosarcoma [58]. In patients with squamous cell carcinoma of the oral tongue, high immune cytolytic activity was associated with a better prognosis [40]. Parainflammation is a procarcinogenic inflammatory process which could be blocked by NSAIDs [42]. Patients characterized by both high TMB and low-risk scores exhibited a heightened survival rate compared to their counterparts, while MDSC and CAF were negatively associated with survival. Previous study has also demonstrated the involvement of MDSC and CAF in tumor immune evasion in hepatocellular carcinoma [59].

Despite the comprehensive evaluation of our models, their construction and validation relied on existing data from a publicly available database, which introduces certain limitations. It is imperative to conduct further external and practical testing to validate the precise predictive efficacy of our models for clinical patients.

In conclusion, this study provides valuable insight into the prognosis of patients with lung adenocarcinoma. We have a preliminary understanding of the correlation between CTLA-4 related lncRNAs and tumor progression and the mechanism. The effect of nitrogen metabolism on the tumor microenvironment of lung adenocarcinoma deserves in-depth study. The innovative prognostic model we developed based on CTLA-4-associated lncRNA has strong predictive power for the overall survival of LUAD patients. This has the potential to guide future diagnosis and treatment of LUAD.

Supplementary Information

The online version contains supplementary material available at <https://doi.org/10.1186/s12885-024-12777-7>.

Supplementary Material 1

Authors' contributions

Huishi Shan performed the statistical analyses and wrote the first draft of the manuscript. Yiting Zhou and Liuhan Mao assisted with the statistical analysis. Xiaocong Wang, Fei Yin and Caixin Liu performed the literature search and discussed the results. Xiao Zhu checked the statistical accuracy as an expert in statistics. Caixin Liu and Xiao Zhu supervised the manuscript. All authors read and approved the final manuscript.

Funding

No funding.

Availability of data and materials

All data generated or analyzed during this study are included in this published article. The datasets used and/or analyzed during the current study are available from the corresponding author upon reasonable request. We welcome legitimate requests for raw data.

Declarations

Ethics approval and consent to participate

This is a retrospective study utilizing publicly available databases, and ethical standards were adhered to by the developers of these databases. The study aligns with the principles of medical research ethics as outlined in the Helsinki Declaration. Given that patient data was extracted from public databases, informed consent forms were not deemed necessary for this study.

Consent for publication

Not applicable.

Competing interests

The authors declare no competing interests.

Author details

¹Department of Clinical Laboratory, The First Affiliated Hospital of Wannan Medical College (Yijishan Hospital of Wannan Medical College), Wuhu, China.

²Department of Radiation Oncology, Guangdong Second People's Hospital, Jinan University, Guangzhou, China. ³Department of Pathology, Qingdao Municipal Hospital Group, Qingdao, China. ⁴Department of Clinical Laboratory, Qingdao Sixth People's Hospital, Qingdao, China. ⁵The Second Affiliated Hospital, Guangdong Medical University, Zhanjiang, China. ⁶Department of Internal Medicine, The Seventh Affiliated Hospital of Sun Yat-Sen University, Shenzhen, China. ⁷The Marine Biomedical Research Institute of Guangdong Zhanjiang, School of Ocean and Tropical Medicine, Guangdong Medical University, Zhanjiang, China.

Received: 12 April 2024 Accepted: 7 August 2024

Published online: 14 August 2024

References

- Rowshanravan B, Halliday N, Sansom DM. CTLA-4: a moving target in immunotherapy. *Blood*. 2018;131(1):58–67.
- Tan S, Li D, Zhu X. Cancer immunotherapy: Pros, cons and beyond. *Biomed Pharmacother*. 2020;124: 109821.
- Wu Z, Li S, Zhu X. The Mechanism of Stimulating and Mobilizing the Immune System Enhancing the Anti-Tumor Immunity. *Front Immunol*. 2021;12:682435.
- Zhang H, Dai Z, Wu W, Wang Z, Zhang N, Zhang L, Zeng WJ, Liu Z, Cheng Q. Regulatory mechanisms of immune checkpoints PD-L1 and CTLA-4 in cancer. *Journal of experimental & clinical cancer research* : CR. 2021;40(1):184.
- Rotte A. Combination of CTLA-4 and PD-1 blockers for treatment of cancer. *Journal of experimental & clinical cancer research* : CR. 2019;38(1):255.
- Reck M, Ciuleanu TE, Cobo M, Schenker M, Zurawski B, Menezes J, Richardt E, Bannouna J, Felip E, Juan-Vidal O, et al. First-line nivolumab plus ipilimumab with two cycles of chemotherapy versus chemotherapy alone (four cycles) in advanced non-small-cell lung cancer: CheckMate 9LA 2-year update. *ESMO open*. 2021;6(5): 100273.
- Walk EE, Yohe SL, Beckman A, Schade A, Zutter MM, Pfeifer J, Berry AB. The Cancer Immunotherapy Biomarker Testing Landscape. *Arch Pathol Lab Med*. 2020;144(6):706–24.
- Bodor JN, Bumber Y, Borghaei H. Biomarkers for immune checkpoint inhibition in non-small cell lung cancer (NSCLC). *Cancer*. 2020;126(2):260–70.
- Lech G, Slotwiński R, Słodkowski M, Krasnodębski IW. Colorectal cancer tumour markers and biomarkers: Recent therapeutic advances. *World J Gastroenterol*. 2016;22(5):1745–55.
- Pennell NA, Arcila ME, Gandara DR, West H. Biomarker Testing for Patients With Advanced Non-Small Cell Lung Cancer: Real-World Issues and Tough Choices. *American Society of Clinical Oncology educational book American Society of Clinical Oncology Annual Meeting*. 2019;39:531–42.
- Zou Z, Zhang M, Xu S, Zhang Y, Zhang J, Li Z, Zhu X. Computational identification of long non-coding RNAs associated with graphene therapy in glioblastoma multiforme. *Brain Commun*. 2024;6(1):fcad293.
- Ye W, Li H, Zhao J, Lu D, Tao T, Zhu X. Graphene therapy-related lncRNAs as prognostic and immune microenvironmental biomarkers in hepatocellular carcinoma. *Transl Oncol*. 2024;43:101915.
- Dong J, Tao T, Yu J, Shan H, Liu Z, Zheng G, Li Z, Situ W, Zhu X, Li Z. A ferroptosis-related lncRNAs signature for predicting prognosis and screening potential therapeutic drugs in patients with lung adenocarcinoma: A retrospective study. *Cancer Rep (Hoboken)*. 2024;7(1): e1925.
- Zhang J, Song L, Li G, Liang A, Cai X, Huang Y, Zhu X, Zhou X. Comprehensive assessment of base excision repair (BER)-related lncRNAs as prognostic and functional biomarkers in lung adenocarcinoma: implications for personalized therapeutics and immunomodulation. *J Cancer Res Clin Oncol*. 2023;149(19):17199–213.
- Yu J, Lan L, Liu C, Zhu X. Improved prediction of prognosis and therapy response for lung adenocarcinoma after identification of DNA-directed RNA polymerase-associated lncRNAs. *J Cancer Res Clin Oncol*. 2023;149(14):12737–54.
- Peng Z, Su P, Yang Y, Yao X, Zhang Y, Jin F, Yang B. Identification of CTLA-4 associated with tumor microenvironment and competing interactions in triple negative breast cancer by co-expression network analysis. *J Cancer*. 2020;11(21):6365–75.
- Baker EJ, Jay JJ, Bubier JA, Langston MA, Chesler EJ. GeneWeaver: a web-based system for integrative functional genomics. *Nucleic Acids Res*. 2012;40(Database issue):D1067-1076.
- Wu Y, He H, Zheng K, Qin Z, Cai N, Zuo S, Zhu X. RNA M6A modification shaping cutaneous melanoma tumor microenvironment and predicting immunotherapy response. *Pigment Cell Melanoma Res*. 2024;37(4):496–509.
- Wei C, Tao T, Zhou J, Zhu X. Leveraging a genomic instability-derived signature to predict the prognosis and therapy sensitivity of clear cell renal cell carcinoma. *Clin Genitourin Cancer*. 2024;22(2):134-148.e138.
- Xiong Z, Han Z, Pan W, Zhu X, Liu C. Correlation between chromatin epigenetic-related lncRNA signature (CELncSig) and prognosis, immune microenvironment, and immunotherapy in non-small cell lung cancer. *PLoS ONE*. 2023;18(5):e0286122.
- Lin Q, Zhang M, Kong Y, Huang Z, Zou Z, Xiong Z, Xie X, Cao Z, Situ W, Dong J, et al. Risk score = lncRNAs associated with doxorubicin metabolism can be used as molecular markers for immune microenvironment and immunotherapy in non-small cell lung cancer. *Heliyon*. 2023;9(3): e13811.
- Liang B, Ding H, Huang L, Luo H, Zhu X. GWAS in cancer: progress and challenges. *Mol Genet Genomics*. 2020;295(3):537–61.
- Goodman AM, Kato S, Bazhenova L, Patel SP, Frampton GM, Miller V, Stephens PJ, Daniels GA, Kurzrock R. Tumor Mutational Burden as an Independent Predictor of Response to Immunotherapy in Diverse Cancers. *Mol Cancer Ther*. 2017;16(11):2598–608.
- Benci JL, Johnson LR, Choa R, Xu Y, Qiu J, Zhou Z, Xu B, Ye D, Nathanson KL, June CH, et al. Opposing Functions of Interferon Coordinate Adaptive and Innate Immune Responses to Cancer Immune Checkpoint Blockade. *Cell*. 2019;178(4):933-948.e914.
- Pietrantonio F, Miceli R, Raimondi A, Kim YW, Kang WK, Langley RE, Choi YY, Kim KM, Nankivell MG, Morano F, et al. Individual Patient Data Meta-Analysis of the Value of Microsatellite Instability As a Biomarker in Gastric

- Cancer. *Journal of clinical oncology : official journal of the American Society of Clinical Oncology*. 2019;37(35):3392–400.
26. Yu H, Boyle TA, Zhou C, Rimm DL, Hirsch FR. PD-L1 Expression in Lung Cancer. *Journal of thoracic oncology : official publication of the International Association for the Study of Lung Cancer*. 2016;11(7):964–75.
 27. Oshi M, Asaoka M, Tokumaru Y, Yan L, Matsuyama R, Ishikawa T, Endo I, Takabe K. CD8 T Cell Score as a Prognostic Biomarker for Triple Negative Breast Cancer. *Int J Mol Sci*. 2020;21(18):6968.
 28. Tcyganov E, Mastio J, Chen E, Gabrilovich DI. Plasticity of myeloid-derived suppressor cells in cancer. *Curr Opin Immunol*. 2018;51:76–82.
 29. Sahai E, Atsaturou I, Cukierman E, DeNardo DG, Egeblad M, Evans RM, Fearon D, Gretchen FR, Hingorani SR, Hunter T, et al. A framework for advancing our understanding of cancer-associated fibroblasts. *Nat Rev Cancer*. 2020;20(3):174–86.
 30. Wu K, Lin K, Li X, Yuan X, Xu P, Ni P, Xu D. Redefining Tumor-Associated Macrophage Subpopulations and Functions in the Tumor Microenvironment. *Front Immunol*. 2020;11:1731.
 31. Hemani G, Zheng J, Elsworth B, Wade KH, Haberland V, Baird D, Laurin C, Burgess S, Bowden J, Langdon R, et al. The MR-Base platform supports systematic causal inference across the human phenome. *eLife*. 2018;7:e34408.
 32. Zhao J, Ming J, Hu X, Chen G, Liu J, Yang C. Bayesian weighted Mendelian randomization for causal inference based on summary statistics. *Bioinformatics (Oxford, England)*. 2020;36(5):1501–8.
 33. Yan J, Ma N, Liu KQ, Qiao TT, Wang Y, Xue JX, Hao XQ, Zheng MD. Network pharmacology analysis of the mechanism of Huisheng oral liquid in the treatment of lung cancer. *Transl Cancer Res*. 2022;11(9):3287–97.
 34. Liu Y, Liu C, Huang D, Ge C, Chen L, Fu J, Du J. Identification and prognostic analysis of candidate biomarkers for lung metastasis in colorectal cancer. *Medicine (Baltimore)*. 2024;103(11):e37484.
 35. Dai W, Guo C, Wang Y, Li Y, Xie R, Wu J, Yao B, Xie D, He L, Li Y, et al. Identification of hub genes and pathways in lung metastatic colorectal cancer. *BMC Cancer*. 2023;23(1):323.
 36. Friedl P, Alexander S. Cancer invasion and the microenvironment: plasticity and reciprocity. *Cell*. 2011;147(5):992–1009.
 37. Kodama M, Oshikawa K, Shimizu H, Yoshioka S, Takahashi M, Izumi Y, Bamba T, Tateishi C, Tomonaga T, Matsumoto M, Nakayama KI. A shift in glutamine nitrogen metabolism contributes to the malignant progression of cancer. *Nat Commun*. 2020;11(1):1320.
 38. Pavlova NN, Thompson CB. The Emerging Hallmarks of Cancer Metabolism. *Cell Metab*. 2016;23(1):27–47.
 39. Bindea G, Mlecnik B, Tosolini M, Kirilovsky A, Waldner M, Obenauf AC, Angell H, Fredriksen T, Lafontaine L, Berger A, et al. Spatiotemporal dynamics of intratumoral immune cells reveal the immune landscape in human cancer. *Immunity*. 2013;39(4):782–95.
 40. Gu X, Boldrup L, Coates PJ, Fahraeus R, Wang L, Wilms T, Norberg-Spaak L, Sgaramella N, Nylander K. High immune cytolytic activity in tumor-free tongue tissue confers better prognosis in patients with squamous cell carcinoma of the oral tongue. *J Pathol Clin Res*. 2019;5(4):240–7.
 41. McGranahan N, Rosenthal R, Hiley CT, Rowan AJ, Watkins TBK, Wilson GA, Birkbak NJ, Veeriah S, Van Loo P, Herrero J, Swanton C. Allele-Specific HLA Loss and Immune Escape in Lung Cancer Evolution. *Cell*. 2017;171(6):1259–1271.e1211.
 42. Pribluda A, Elyada E, Wiener Z, Hamza H, Goldstein RE, Biton M, Burstain I, Morgenstern Y, Brachya G, Billauer H, et al. A senescence-inflammatory switch from cancer-inhibitory to cancer-promoting mechanism. *Cancer Cell*. 2013;24(2):242–56.
 43. Wang H, Shi Y, Xu X, Xu S, Shi Y, Chen W, Wang K. A novel neutrophil extracellular traps-related lncRNA signature predicts prognosis in patients with early-stage lung adenocarcinoma. *Ann Med*. 2023;55(2):2279754.
 44. Hu B, Zou T, Qin W, Shen X, Su Y, Li J, Chen Y, Zhang Z, Sun H, Zheng Y, et al. Inhibition of EGFR Overcomes Acquired Lenvatinib Resistance Driven by STAT3-ABC1 Signaling in Hepatocellular Carcinoma. *Cancer Res*. 2022;82(20):3845–57.
 45. LaRocca JL, Rasoulpour RJ, Gollapudi BB, Eisenbrandt DL, Murphy LA, LeBaron MJ. Integration of novel approaches demonstrates simultaneous metabolic inactivation and CAR-mediated hepatocarcinogenesis of a nitrification inhibitor. *Toxicol Rep*. 2017;4:586–97.
 46. Murphy L, LeBaron MJ, Johnson K, Rasoulpour RJ, Wang X, LaRocca J. Bridging Sex-Specific Differences in the CAR-Mediated Hepatocarcinogenesis of Nitrapyrin Using Molecular and Apical End-points. *Frontiers in toxicology*. 2021;3:766196.
 47. Li Y, Yi Y, Gao X, Wang X, Zhao D, Wang R, Zhang LS, Gao B, Zhang Y, Zhang L, et al. 2'-O-methylation at internal sites on mRNA promotes mRNA stability. *Mol Cell*. 2024;84(12):2320–2336.e2326.
 48. Li Y, Yi Y, Lv J, Gao X, Yu Y, Babu SS, Bruno I, Zhao D, Xia B, Peng W, et al. Low RNA stability signifies increased post-transcriptional regulation of cell identity genes. *Nucleic Acids Res*. 2023;51(12):6020–38.
 49. Zhu J, Zhu S, Yu Q, Wu Y. LncRNA FAM66C inhibits pancreatic cancer progression by sponging miR-574-3p. *Transl Cancer Res*. 2020;9(3):1806–17.
 50. Xie Y, Gu J, Qin Z, Ren Z, Wang Y, Shi H, Chen B. Long non-coding RNA FAM66C is associated with clinical progression and promotes cell proliferation by inhibiting proteasome pathway in prostate cancer. *Cell Biochem Funct*. 2020;38(8):1006–16.
 51. Zhang X, Yu K, Ma L, Qian Z, Tian X, Miao Y, Niu Y, Xu X, Guo S, Yang Y, et al. Endogenous glutamate determines ferroptosis sensitivity via ADCY10-dependent YAP suppression in lung adenocarcinoma. *Theranostics*. 2021;11(12):5650–74.
 52. Munder M, Engelhardt M, Knies D, Medenhoff S, Wabnitz G, Luckner-Minden C, Feldmeyer N, Voss RH, Kropf P, Müller I, et al. Cytotoxicity of tumor antigen specific human T cells is unimpaired by arginine depletion. *PLoS ONE*. 2013;8(5):e63521.
 53. Xie S, Wu Z, Qi Y, Wu B, Zhu X. The metastasizing mechanisms of lung cancer: Recent advances and therapeutic challenges. *Biomed Pharmacother*. 2021;138:111450.
 54. Xu P, Luo H, Kong Y, Lai WF, Cui L, Zhu X. Cancer neoantigen: Boosting immunotherapy. *Biomed Pharmacother*. 2020;131:110640.
 55. Lin B, Du L, Li H, Zhu X, Cui L, Li X. Tumor-infiltrating lymphocytes: Warriors fight against tumors powerfully. *Biomed Pharmacother*. 2020;132:110873.
 56. Bell HN, Huber AK, Singhal R, Korimerla N, Rebernick RJ, Kumar R, El-Derany MO, Sajjakulnukit P, Das NK, Kerk SA, et al. Microenvironmental ammonia enhances T cell exhaustion in colorectal cancer. *Cell Metab*. 2023;35(1):134–149.e136.
 57. Spinelli JB, Yoon H, Ringel AE, Jeanfavre S, Clish CB, Haigis MC. Metabolic recycling of ammonia via glutamate dehydrogenase supports breast cancer biomass. *Science*. 2017;358(6365):941–6.
 58. Zheng D, Wei Z, Guo W. Identification of a Solute Carrier Family-Based Signature for Predicting Overall Survival in Osteosarcoma. *Front Genet*. 2022;13:849789.
 59. Lurje I, Werner W, Mohr R, Roderburg C, Tacke F, Hammerich L. In Situ Vaccination as a Strategy to Modulate the Immune Microenvironment of Hepatocellular Carcinoma. *Front Immunol*. 2021;12:650486.

Publisher's Note

Springer Nature remains neutral with regard to jurisdictional claims in published maps and institutional affiliations.